Well-Conditioned CFIE for Scattering from Dielectric Coated Conducting Bodies above a Half-Space

Dazhi Ding, Jinmin Ge, and Rushan Chen

Department of Communication Engineering
Nanjing University of Science and Technology, Nanjing, 210094, China
dzding@mail.njust.edu.cn

Abstract ─ In this paper, a well-conditioned coupled combined-field integral equation called the electric and magnetic current combined-field integral equation (JCFIE-JMCFIE) is proposed for the analysis of electromagnetic scattering from coated targets above a lossy half-space. The half-space multilevel fast multipole algorithm (MLFMA) is used to reduce computational complexity. The inner-outer flexible generalized minimal residual method (FGMRES) was used as the iterative solver to further speed up the convergence rate. Numerical results were presented to demonstrate the accuracy and efficiency of the proposed method.

Index Terms ─ Electric and magnetic current combined-field integral equation (JMCFIE), flexible generalized minimal residual method (FGMRES), half-space, multilevel fast multipole algorithm (MLFMA).

I. INTRODUCTION

There is significant interest in scattering from conducting bodies coated with dielectric materials situated in the presence of a lossy half-space [1-5]. It has applications in many domains such as communications, target identification, and so on. One of the principal tools for the analysis of such scattering is the method of moments (MoM) [6]. The electromagnetic integral equation is first discretized into a matrix equation using the Galerkin-based MoM with subdomain basis functions such as Rao–Wilton–Glisson (RWG) functions [7] for triangular patches. When iterative solvers are used to solve the MoM matrix equation; the fast multipole algorithm (FMA) or multilevel fast multipole algorithm (MLFMA) [8-11] can be used to accelerate the calculation of matrix–vector products. The half-space MLFMA differs from the free-space MLFMA. In half-space MLFMA, the near interaction terms are evaluated efficiently via the discrete complex-image method (DCIM) [12, 13]. The far interaction terms are evaluated efficiently by employing the asymptotic form of the dyadic Green's function. Each component of the approximate Green's function is expressed in terms of the direct-radiation term plus radiation from an image source in real space [14]. The former accounts for the radiation of currents into the medium in which it resides, while the latter accounts for interactions with the half-space interface. The half-space MLFMA remains the same computational complexity of O(NlogN) both in RAM and computational requirement (per iteration) as free-space MLFMA.

Although the calculation complexity and memory will be decreased in MLFMA, the number of iterations needed to achieve desired precision cannot be reduced. Actually the number of iterations largely depends on the spectral properties of the integral operator or the distribution of the impedance matrix's eigenvalues. To effectively reduce the number of iterations, there are mainly two methods. One is to construct a new integral equation leading to a well-conditioned matrix equation. The other is to use fast iteration techniques and efficient preconditioning techniques to reduce the condition number of the operator equations. Researchers have investigated various integral equations for 3D coated conducting objects [15-17]. Employing the surface equivalence principle, the problem is formulated in terms of a set of coupled integral equations involving equivalent electric and magnetic surface currents which represent boundary fields. The most familiar formulation for

this problem is the Poggio-Miller-Chang-Harrington-Wu-Tsai (PMCHWT) integral equation combined with electric field integral equation (EFIE) [18]. The PMCHWT formulation belongs to the integral equations of the first kind and it is found to be free of interior resonances and yields accurate and stable solutions; however, its iteration convergence rate is found to be slow [17]. To solve this problem, a new electric and magnetic current combined-field integral equation (JMCFIE) is developed leading to a well tested system with the RWG basis functions and Galerkin's method for scattering problems in free-space [16, 19-20]. Özgür Ergül and Levent Gürel have, also, applied the JMCFIE formulation with MLFMA for fast analysis of scattering from dielectric objects [19]. Researchers have, also, developed efficient iteration techniques and robust preconditioning techniques for the Krylov subspace iterative methods; among which, the GMRES (generalized minimal residual) method proposed in [21] is the most popular and efficient method for the iterative solution of sparse linear systems with an unsymmetric nonsingular matrix. For the GMRES algorithm, this can be easily accomplished with the help of a rather simple modification of the standard algorithm, referred to as the inner-outer flexible generalized minimum residual method (FGMRES) [21-24]. An important property of FGMRES is that it satisfies the residual norm minimization property over the preconditioned Krylov subspace just as in the standard GMRES algorithm.

The objective of this paper is to achieve a fast and accurate solution to the electromagnetic wave scattering from an arbitrary shaped coated conducting target situated in the presence of a lossy half-space. In this paper, we extended the JMCFIE method combined with MLFMA to efficiently analyze electromagnetic scattering from coated targets above a lossy half-space. This paper is outlined as follows. Section 2 gives an introduction of well-conditioned coupled surface integral equation. Numerical examples are given to demonstrate the accuracy and efficiency of the proposed method in radar cross section (RCS) calculations in Section 3. Section 4 gives some conclusions.

II. FORMULATION AND THEORY

As shown in Figure 1, the configuration of an arbitrarily shaped conducting body coated with dielectric materials in half-space. The dielectric parameters of space are $(\varepsilon_1, \mu_1, \sigma_1)$ and $(\varepsilon_{\text{half}}, \mu_{half}, \sigma_{half})$. As shown in Figure 1, the dielectric surface is S_d, and the metallic surface is S_c. The composite structure is illuminated by an incident plane wave (E^{inc}, H^{inc}). By invoking the equivalence principle [18], two equivalent problems are formulated, each valid for regions external and internal to the dielectric material as shown in Figure 1.

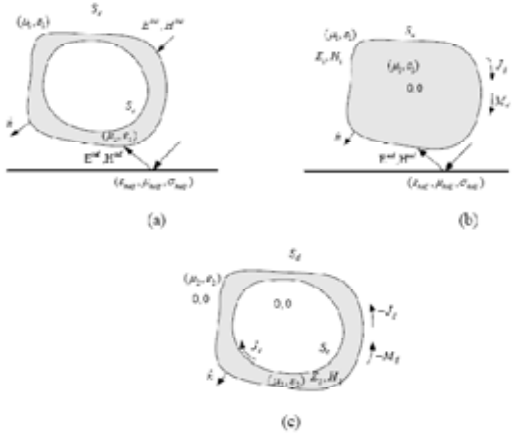

Fig. 1. Configuration of an arbitrarily shaped conducting body coated with dielectric materials (a) original problem (b) outer problem (c) inner problem.

In the equivalence problem for the external region, dielectric surface S_d is replaced by a fictitious mathematical surface. The entire space is filled with external medium $(\varepsilon_1, \mu_1, \sigma_1)$. The field inside the surface S_d is set to zero. Equivalent electric current $\mathbf{J}_d$ and equivalent magnetic current $\mathbf{M}_d$ are presented on S_d. The so-called T equations T-EFIE$_1$ and T-MFIE$_1$ for the exterior equivalent problem can be derived by taking the tangential boundary continuity conditions on the object's surface [18]:

$$\left(\mathbf{E}_1^{inc} + \mathbf{E}_1^{ref}\right)\Big|_{\tan} = \left[-\mathbf{E}_1^{s}\right]\Big|_{\tan} \tag{1}$$

$$\left(\mathbf{H}_1^{inc} + \mathbf{H}_1^{ref}\right)\Big|_{\tan} = \left[-\mathbf{H}_1^{s}\right]\Big|_{\tan} \tag{2}$$

$$\begin{aligned}\mathbf{E}_1^s = -(&j\omega\mu_1 \int_{T'} \bar{\bar{\mathbf{K}}}^A \cdot \mathbf{J}_d dS' - \frac{\nabla}{j\omega\varepsilon_1}\int_{T'} K^{\phi e}\nabla_s' \cdot \mathbf{J}_d dS' \\ &- \int_{T'} \bar{\bar{\mathbf{G}}}^{EM} \cdot \mathbf{M}_d dS' + \frac{1}{2}\mathbf{n}_1 \times \mathbf{M}_d)\end{aligned} \tag{3}$$

$$\mathbf{H}_1^s = -(j\omega\varepsilon_1\int_{T'}\bar{\bar{\mathbf{K}}}^F\cdot\mathbf{M}_d dS' - \frac{\nabla}{j\omega\mu_1}\int_{T'}K^{\phi m}\nabla_s'\cdot\mathbf{M}_d dS' - \int_{T'}\bar{\bar{\mathbf{G}}}^{HJ}\cdot\mathbf{J}_d dS' + \frac{1}{2}\mathbf{n}_1\times\mathbf{J}_d), \tag{4}$$

where the half-space Green's functions $\bar{\bar{\mathbf{K}}}^A$ $\bar{\bar{\mathbf{K}}}^F$ are for the vector potentials and $K^{\phi e}$ $K^{\phi m}$ are for the scalar potentials, meanwhile, $\bar{\bar{\mathbf{G}}}^{EM}$ is dyadic Green's function for electric field due to magnetic currents and $\bar{\bar{\mathbf{G}}}^{HJ}$ is for magnetic field due to electric current. For detailed spectral domain expressions of these half-space Green's functions please refer to [25]. In general, the spatial domain Green's functions are expressed in terms of Sommerfeld integrals. Due to the highly oscillatory nature of the integrand, numerical integration is very time consuming. In this paper, a two-level generalized pencil of function (GPOF) method is utilized to realize DCIM [13]. In the two-level GPOF, dense sampling is adopted to get full information in the quick variant area where k_ρ is relative small, while a sparse sampling in the slow variant area. In this way, high precision can be realized with fewer samples [13]. Then the spatial domain Green's functions can be obtained in closed forms from their spectral-domain counterparts via the Sommerfeld identity. By operating with $\hat{\mathrm{n}}_1\times$ to (1) and (2) on the object's surface the so-called N equations, N-EFIE$_1$ and N-MFIE$_1$, for the exterior equivalent problem can be derived

$$\mathbf{n}_1\times\left(\mathbf{E}_1^{inc}+\mathbf{E}_1^{ref}\right)=\mathbf{n}_1\times\left(-\mathbf{E}_1^s\right) \tag{5}$$

$$\mathbf{n}_1\times\left(\mathbf{H}_1^{inc}+\mathbf{H}_1^{ref}\right)=\mathbf{n}_1\times\left(-\mathbf{H}_1^s\right). \tag{6}$$

In the equivalence problem for the interior region in Figure 1(c), the medium outside is given the same material parameters $(\varepsilon_2,\mu_2,\sigma_2)$ as the coated dielectric medium. The conducting surfaces located inside the dielectric body are also replaced by fictitious mathematical surfaces. The equivalent electric current $-\mathbf{J}_d$ and equivalent magnetic current $-\mathbf{M}_d$ are presented on S_d. The equivalent current $\mathbf{J}_c$ is introduced on the conducting surface S_c. Based on the boundary conditions, T-EFIE$_2$ and T-MFIE$_2$ are presented:

On dielectric surface S_d:

$$\mathbf{E}_2^{inc}\big|_{\tan}=\left(-\mathbf{E}_2^s\right)\big|_{\tan} \tag{7}$$

$$\mathbf{H}_2^{inc}\big|_{\tan}=\left(-\mathbf{H}_2^s\right)\big|_{\tan}. \tag{8}$$

On metallic surface S_c:

$$\mathbf{E}_2^{inc}\big|_{\tan}=\left(-\mathbf{E}_2^s\right)\big|_{\tan} \tag{9}$$

$$\mathbf{E}_2^s=-\begin{pmatrix} j\omega\mu_2\int_{T'}g_2\cdot(-\mathbf{J}_d)dS'-\frac{\nabla}{j\omega\varepsilon_2}\int_{T'}g_2\nabla_s'\cdot(-\mathbf{J}_d)dS'+\int_{T'}\nabla g_2\times(-\mathbf{M}_d)dS' \\ +\frac{1}{2}\mathbf{n}_2\times(-\mathbf{M}_d)+j\omega\mu_2\int_{T'}g_2\cdot(\mathbf{J}_c)dS'-\frac{\nabla}{j\omega\varepsilon_2}\int_{T'}g_2\nabla_s'\cdot(\mathbf{J}_c)dS' \end{pmatrix} \tag{10}$$

$$\mathbf{H}_2^s=-\begin{pmatrix} j\omega\varepsilon_2\int_{T'}g_2\cdot(-\mathbf{M}_d)dS'-\frac{\nabla}{j\omega\mu_2}\int_{T'}g_2\nabla_s'\cdot(-\mathbf{M}_d)dS' \\ -\int_{T'}\nabla g_2\times(-\mathbf{J}_d)dS'-\frac{1}{2}\mathbf{n}_2\times(-\mathbf{J}_d)-\int_{T'}\nabla g_2\times(\mathbf{J}_c)dS'-\frac{1}{2}\mathbf{n}_2\times(\mathbf{J}_c) \end{pmatrix}, \tag{11}$$

where g_2 is the Green's function of infinity dielectric free-space. By operating with $\hat{\mathrm{n}}_2\times$ to (7), (8), and (9), N-EFIE$_2$ and N-MFIE$_2$ for the exterior equivalent problem can be derived:

On dielectric surface S_d:

$$\mathbf{n}_2\times\mathbf{E}_2^{inc}=\mathbf{n}_2\times\left(-\mathbf{E}_2^s\right) \tag{12}$$

$$\mathbf{n}_2\times\mathbf{H}_2^{inc}=\mathbf{n}_2\times\left(-\mathbf{H}_2^s\right). \tag{13}$$

On metallic surface S_c:

$$\mathbf{n}_2\times\mathbf{E}_2^{inc}=\mathbf{n}_2\times\left(-\mathbf{E}_2^s\right). \tag{14}$$

Note that $\hat{\mathrm{n}}_1=-\hat{\mathrm{n}}_2=\hat{\mathrm{n}}$. The negative sign is due to the direction of the unit normal vector pointing into the external medium.

A. EFIE-PMCHWT2 formulation for scattering problems in half-space

Using formulation (1)-(2), (7)-(9), the traditional PMCHWT combined with EFIE can be formed as follows:

$$\begin{cases}\text{T-EFIE}_2\\ \text{T-EFIE}_1-\text{T-EFIE}_2\\ \text{T-MFIE}_1-\text{T-MFIE}_2\end{cases}. \tag{15}$$

After it is expanded and tested with the RWG basis functions $\mathbf{f}_n$, a matrix equation will be:

$$\begin{bmatrix}\left[Z_{mn}^{J_cJ_c}\right] & \left[Z_{mn}^{J_cJ_d}\right] & \left[T_{mn}^{J_cM_d}\right]\\ \left[Z_{mn}^{J_dJ_c}\right] & \left[Z_{mn}^{J_dJ_d}\right] & \left[T_{mn}^{J_dM_d}\right]\\ \left[T_{mn}^{M_dJ_c}\right] & \left[T_{mn}^{M_dJ_d}\right] & \left[Y_{mn}^{M_dM_d}\right]\end{bmatrix}\begin{bmatrix}I_{cn}\\ I_{dn}\\ M_{dn}\end{bmatrix}=\begin{bmatrix}V_{cm}\\ V_{dm}\\ H_{dm}\end{bmatrix}. \tag{16}$$

In the equation, V_{cm}, V_{dm}, and H_{dm} is the incident field and reflect field summation. $\mathbf{J}_d=\sum_{n=1}^{N_d}I_{dn}\mathbf{f}_n$ 、

$\mathbf{J}_c = \sum_{n=1}^{N_c} I_{cn}\mathbf{f}_n$, $\mathbf{M}_d = \eta_0 \sum_{n=1}^{N_d} M_{dn}\mathbf{f}_n$, I_{dn}, I_{cn}, M_{dn} are the current coefficients needed to solve. To improve the condition number of the matrix, a coefficient adjustment is made to form the PMCHWT2 formulation:

$$\begin{bmatrix} \left[Z_{mn}^{J_cJ_c}\right] & \left[Z_{mn}^{J_cJ_d}\right] & \eta_1\left[T_{mn}^{J_cM_d}\right] \\ \left[Z_{mn}^{J_dJ_c}\right] & \left[Z_{mn}^{J_dJ_d}\right] & \eta_1\left[T_{mn}^{J_dM_d}\right] \\ \eta_1\left[T_{mn}^{M_dJ_c}\right] & \eta_1\left[T_{mn}^{M_dJ_d}\right] & \eta_1^2\left[Y_{mn}^{M_dM_d}\right] \end{bmatrix} \begin{bmatrix} I_{cn} \\ I_{dn} \\ M_{dn}/\eta_1 \end{bmatrix} = \begin{bmatrix} V_{cm} \\ V_{dm} \\ \eta_1 H_{dm} \end{bmatrix}, \tag{17}$$

where the $\eta_1 = \sqrt{\mu_1/\varepsilon_1}$.

B. JCFIE-JMCFIE formulation for scattering problems in half-space

In this paper, the novel integral equation JMCFIE [16] combined with JCFIE is extended to the half-space situation to realize accurate and fast solution of scattering from coated conducting targets. The JMCFIE formulation combined with JCFIE for half-space problems can be obtained by combining the T and N equations as the following form:

$$\begin{cases} -\dfrac{1}{\eta_2}\text{T-EFIE}_2 - \text{N-MFIE}_2 \\ \dfrac{1}{\eta_1}\text{T-EFIE}_1 - \dfrac{1}{\eta_2}\text{T-EFIE}_2 + \text{N-MFIE}_1 - \text{N-MFIE}_2 \\ \eta_1\text{T-MFIE}_1 - \eta_2\text{T-MFIE}_2 - \text{N-EFIE}_1 + \text{N-EFIE}_2 \end{cases}. \tag{18}$$

After expanding the unknowns $\mathbf{J}_c$, $\mathbf{J}_d$, and $\mathbf{M}_d$ in (18) with the RWG basis functions and using the Galerkin's method, a well-conditioned matrix equation will be:

$$\begin{bmatrix} \left[Z_{mn}^{J_cJ_c}\right] & \left[Z_{mn}^{J_cJ_d}\right] & \left[T_{mn}^{J_cM_d}\right] \\ \left[Z_{mn}^{J_dJ_c}\right] & \left[Z_{mn}^{J_dJ_d}\right] & \left[T_{mn}^{J_dM_d}\right] \\ \left[T_{mn}^{M_dJ_c}\right] & \left[T_{mn}^{M_dJ_d}\right] & \left[Y_{mn}^{M_dM_d}\right] \end{bmatrix} \begin{bmatrix} I_{cn} \\ I_{dn} \\ M_{dn} \end{bmatrix} = \begin{bmatrix} F_{ecm} \\ F_{edm} \\ F_{hdm} \end{bmatrix}. \tag{19}$$

$$\begin{aligned} Z_{mn}^{J_dJ_d} = {} & \frac{1}{\eta_1} j\omega\mu_1 \left\langle \int_{T'} \bar{\bar{\mathbf{K}}}^A \cdot \mathbf{f}_n dS', \mathbf{f}_m \right\rangle + \frac{1}{\eta_1 j\omega\varepsilon_1} \left\langle \int_{T'} K^{\phi e} \nabla_s' \cdot \mathbf{f}_n dS', \nabla \cdot \mathbf{f}_m \right\rangle \\ & - \left\langle \boldsymbol{n} \times \int_{T'} \bar{\bar{\mathbf{G}}}^{HJ} \cdot \mathbf{f}_n dS', \mathbf{f}_m \right\rangle + \frac{1}{2}\langle \mathbf{f}_n \cdot \mathbf{f}_m \rangle \\ & + \frac{1}{\eta_2} j\omega\mu_2 \left\langle \int_{T'} g_2 \cdot \mathbf{f}_n dS', \mathbf{f}_m \right\rangle + \frac{1}{\eta_2 j\omega\varepsilon_2} \left\langle \int_{T'} g_2 \nabla_s' \cdot \mathbf{f}_n dS', \nabla \cdot \mathbf{f}_m \right\rangle \\ & + \left\langle \boldsymbol{n} \times \int_{T'} \nabla g_2 \times \mathbf{f}_n dS', \mathbf{f}_m \right\rangle + \frac{1}{2}\langle \mathbf{f}_n \cdot \mathbf{f}_m \rangle \end{aligned} \tag{20}$$

$$\begin{aligned} Z_{mn}^{J_dJ_c} = {} & -\frac{1}{\eta_2} j\omega\mu_2 \left\langle \int_{T'} g_2 \cdot \mathbf{f}_n dS', \mathbf{f}_m \right\rangle - \frac{1}{\eta_2 j\omega\varepsilon_2} \left\langle \int_{T'} g_2 \nabla_s' \cdot \mathbf{f}_n dS', \nabla \cdot \mathbf{f}_m \right\rangle \\ & - \left\langle \boldsymbol{n} \times \int_{T'} \nabla g_2 \times \mathbf{f}_n dS', \mathbf{f}_m \right\rangle - \frac{1}{2}\langle \mathbf{f}_n \cdot \mathbf{f}_m \rangle \end{aligned} \tag{21}$$

$$\begin{aligned} T_{mn}^{J_dM_d} = {} & j\omega\varepsilon_1 \left\langle \boldsymbol{n} \times \int_{T'} \bar{\bar{\mathbf{K}}}^F \cdot \mathbf{f}_n dS', \mathbf{f}_m \right\rangle - \frac{1}{j\omega\mu_1} \left\langle \boldsymbol{n} \times \nabla \int_{T'} K^{\phi m} \nabla_s' \cdot \mathbf{f}_n dS', \mathbf{f}_m \right\rangle \\ & - \frac{1}{\eta_1} \left\langle \int_{T'} \bar{\bar{\mathbf{G}}}^{EM} \cdot \mathbf{f}_n dS', \mathbf{f}_m \right\rangle + \frac{1}{2\eta_1} \langle \mathbf{n} \times \mathbf{f}_n, \mathbf{f}_m \rangle \\ & - j\omega\varepsilon_2 \left\langle \boldsymbol{n} \times \int_{T'} g_2 \cdot \mathbf{f}_n dS', \mathbf{f}_m \right\rangle + \frac{1}{j\omega\mu_2} \left\langle \boldsymbol{n} \times \nabla \int_{T'} g_2 \nabla_s' \cdot \mathbf{f}_n dS', \mathbf{f}_m \right\rangle \\ & + \frac{1}{\eta_2} \left\langle \int_{T'} \nabla g_2 \times \mathbf{f}_n dS', \mathbf{f}_m \right\rangle - \frac{1}{2\eta_2} \langle \mathbf{n} \times \mathbf{f}_n, \mathbf{f}_m \rangle \end{aligned} \tag{22}$$

$$Z_{mn}^{J_cJ_d} = \frac{1}{\eta_2} j\omega\mu_2 \left\langle \int_{T'} g_2 \cdot \mathbf{f}_n dS', \mathbf{f}_m \right\rangle + \frac{1}{\eta_2 j\omega\varepsilon_2} \left\langle \int_{T'} g_2 \nabla_s' \cdot \mathbf{f}_n dS', \nabla \cdot \mathbf{f}_m \right\rangle + \left\langle \boldsymbol{n} \times \int_{T'} \nabla g_2 \times \mathbf{f}_n dS', \mathbf{f}_m \right\rangle + \frac{1}{2}\langle \mathbf{f}_n \cdot \mathbf{f}_m \rangle \tag{23}$$

$$Z_{mn}^{J_cJ_c} = -\frac{1}{\eta_2} j\omega\mu_2 \left\langle \int_{T'} g_2 \cdot \mathbf{f}_n dS', \mathbf{f}_m \right\rangle - \frac{1}{\eta_2 j\omega\varepsilon_2} \left\langle \int_{T'} g_2 \nabla_s' \cdot \mathbf{f}_n dS', \nabla \cdot \mathbf{f}_m \right\rangle - \left\langle \boldsymbol{n} \times \int_{T'} \nabla g_2 \times \mathbf{f}_n dS', \mathbf{f}_m \right\rangle - \frac{1}{2}\langle \mathbf{f}_n \cdot \mathbf{f}_m \rangle \tag{24}$$

$$\begin{aligned} T_{mn}^{J_cM_d} = {} & -j\omega\varepsilon_2 \left\langle \boldsymbol{n} \times \int_{T'} g_2 \cdot \mathbf{f}_n dS', \mathbf{f}_m \right\rangle + \frac{1}{j\omega\mu_2} \left\langle \boldsymbol{n} \times \nabla \int_{T'} g_2 \nabla_s' \cdot \mathbf{f}_n dS', \mathbf{f}_m \right\rangle \\ & + \frac{1}{\eta_2} \left\langle \int_{T'} \nabla g_2 \times \mathbf{f}_n dS', \mathbf{f}_m \right\rangle - \frac{1}{2\eta_2} \langle \mathbf{n} \times \mathbf{f}_n, \mathbf{f}_m \rangle \end{aligned} \tag{25}$$

$$\begin{aligned} T_{mn}^{M_dJ_d} = {} & -j\omega\mu_1 \left\langle \boldsymbol{n} \times \int_{T'} \bar{\bar{\mathbf{K}}}^A \cdot \mathbf{f}_n dS', \mathbf{f}_m \right\rangle + \frac{1}{j\omega\varepsilon_1} \left\langle \boldsymbol{n} \times \nabla \int_{T'} K^{\phi e} \nabla_s' \cdot \mathbf{f}_n dS', \mathbf{f}_m \right\rangle \\ & - \eta_1 \left\langle \int_{T'} \bar{\bar{\mathbf{G}}}^{HJ} \cdot \mathbf{f}_n dS', \mathbf{f}_m \right\rangle - \frac{\eta_1}{2} \langle \mathbf{n} \times \mathbf{f}_n, \mathbf{f}_m \rangle \\ & + j\omega\mu_2 \left\langle \boldsymbol{n} \times \int_{T'} g_2 \cdot \mathbf{f}_n dS', \mathbf{f}_m \right\rangle - \frac{1}{j\omega\varepsilon_2} \left\langle \boldsymbol{n} \times \nabla \int_{T'} g_2 \nabla_s' \cdot \mathbf{f}_n dS', \mathbf{f}_m \right\rangle \\ & - \eta_2 \left\langle \int_{T'} \nabla g_2 \times \mathbf{f}_n dS', \mathbf{f}_m \right\rangle + \frac{\eta_2}{2} \langle \mathbf{n} \times \mathbf{f}_n, \mathbf{f}_m \rangle \end{aligned} \tag{26}$$

$$T_{mn}^{M_dJ_c} = -j\omega\mu_2 \left\langle \boldsymbol{n} \times \int_{T'} g_2 \cdot \mathbf{f}_n dS', \mathbf{f}_m \right\rangle + \frac{1}{j\omega\varepsilon_2} \left\langle \boldsymbol{n} \times \nabla \int_{T'} g_2 \nabla_s' \cdot \mathbf{f}_n dS', \mathbf{f}_m \right\rangle + \eta_2 \left\langle \int_{T'} \nabla g_2 \times \mathbf{f}_n dS', \mathbf{f}_m \right\rangle - \frac{\eta_2}{2} \langle \mathbf{n} \times \mathbf{f}_n, \mathbf{f}_m \rangle \tag{27}$$

$$\begin{aligned} Y_{mn}^{M_dM_d} = {} & \eta_1 j\omega\varepsilon_1 \left\langle \int_{T'} \bar{\bar{\mathbf{K}}}^F \cdot \mathbf{f}_n dS', \mathbf{f}_m \right\rangle + \frac{\eta_1}{j\omega\mu_1} \left\langle \int_{T'} K^{\phi m} \nabla_s' \cdot \mathbf{f}_n dS', \nabla \cdot \mathbf{f}_m \right\rangle \\ & + \left\langle \boldsymbol{n} \times \int_{T'} \bar{\bar{\mathbf{G}}}^{EM} \cdot \mathbf{f}_n dS', \mathbf{f}_m \right\rangle + \frac{1}{2}\langle \mathbf{f}_n \cdot \mathbf{f}_m \rangle \\ & + \eta_2 j\omega\varepsilon_2 \left\langle \int_{T'} g_2 \cdot \mathbf{f}_n dS', \mathbf{f}_m \right\rangle + \frac{\eta_2}{j\omega\mu_2} \left\langle \int_{T'} g_2 \nabla_s' \cdot \mathbf{f}_n dS', \nabla \cdot \mathbf{f}_m \right\rangle \\ & + \left\langle \boldsymbol{n} \times \int_{T'} \nabla g_2 \times \mathbf{f}_n dS', \mathbf{f}_m \right\rangle + \frac{1}{2}\langle \mathbf{f}_n \cdot \mathbf{f}_m \rangle \end{aligned} \tag{28}$$

$$F_{ecm} = \left\langle \left(-\frac{1}{\eta_2}\mathbf{E}_2^{inc} + \hat{\mathrm{n}}\times\mathbf{H}_2^{inc} \right), \mathbf{f}_m \right\rangle \quad (29)$$

$$F_{edm} = \left\langle \left(\frac{1}{\eta_1}\mathbf{E}_1^{inc} - \frac{1}{\eta_2}\mathbf{E}_2^{inc} + \hat{\mathrm{n}}\times\mathbf{H}_1^{inc} + \hat{\mathrm{n}}\times\mathbf{H}_2^{inc} \right), \mathbf{f}_m \right\rangle \quad (30)$$

$$F_{hdm} = \left\langle \left(\eta_1\mathbf{H}_1^{inc} - \eta_2\mathbf{H}_2^{inc} - \hat{\mathrm{n}}\times\mathbf{E}_1^{inc} - \hat{\mathrm{n}}\times\mathbf{E}_2^{inc} \right), \mathbf{f}_m \right\rangle. \quad (31)$$

It's obvious that the JCFIE-JMCFIE formulation contains well-tested identity operators. The impedance matrix of JCFIE-JMCFIE is well-conditioned since the well-tested identity operators lead to diagonally-dominant matrices. This is an essential requirement for a formulation with a high convergence rate. This explains why the developed JCFIE-JMCFIE formulation leads to a better conditioned matrix equation than the traditional EFIE-PMCHWT formulations and hence gives more rapidly converging iterative solutions. Finally, the linear system of equations in (19) can be solved by the FGMRES method [21-24] using half-space MLFMA to accelerate the matrix-vector products [8].

III. NUMERICAL EXAMPLES

In this section, we show some numerical results for the electromagnetic characteristics of a conducting body coated with dielectric materials in half-space that illustrate the accuracy and effectiveness of the proposed JCFIE-JMCFIE formulation. The JCFIE-JMCFIE linear systems based on the RWG basis functions are solved with MLFMA accelerated Krylov iterative methods. All numerical experiments are performed on a Pentium 4 with 2.9 GHz CPU and 2GB RAM in single precision. In this paper, the inner-outer FGMRES [21-24] is used as the iterative solver for the JCFIE-JMCFIE and EFIE-PMCHWT2 formulation to accelerate the convergence rate compared with GMRES. In the flowing examples, the inner and outer restart numbers of FGMRES are both 10. The stop precision of restarted GMRES is denoted to be 1.E-4. In the FGMRES algorithm, the stop precision for the inner and outer iteration is 1.E-2, 1.E-4, respectively. Additional details and comments on the implementation are given as follows:

· Zero vector is taken as an initial approximate solution for all examples and all systems in each example.

· The iteration process is terminated when the normalized backward error is reduced by 10^{-4} for all the examples.

At first, the developed formulations are verified by the conducting body coated with dielectric materials in free-space. The first example is a metallic sphere covered with dielectric material in free-space as shown in Fig. 2(a). The metallic sphere's radius is $a_1 = 0.3423\lambda_0$ (λ_0 is the wavelength in free-space). The thickness of the coated dielectric is $a_2 = 0.1017\lambda_0$ and the relative permittivity is with $\varepsilon_r = 4$. The incident angles of plane wave are $\theta_i = 180^\circ$ and $\phi_i = 180^\circ$ at a frequency of $f = 300MHz$. Fig. 2(b) gives the $\theta\theta$ co-polarized bi-static RCS for the above free-space coated metallic sphere solved by the JCFIE-JMCFIE, EFIE-PMCHWT2, and Mie, respectively. The scattering angle is $0^\circ \le \theta_s \le 180^\circ, \phi_s = 0^\circ$. MLFMA with 2 levels is used to accelerate the matrix-vector products. The coated metallic sphere is discretized with 3240 triangular patches leading to 7720 unknowns. It can be found that the results using the JCFIE-JMCFIE, EFIE-PMCHWT2 method are in good agreement with the Mie series solution. Figure 3 shows the convergence rates of the JCFIE-JMCFIE and EFIE-PMCHWT2 formulations solved by GMRES method for the above example. From Fig. 3, it can be found that the EFIE-PMCHWT method does not reach convergence after 700 iteration steps. However, the JCFIE-JMCFIE can reach convergence in 100 iteration steps. It can be concluded that the condition number of the proposed JCFIE-JMCFIE is much better than the EFIE-PMCHWT2.

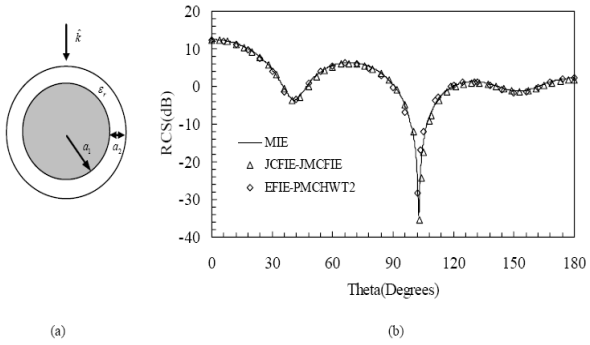

Fig. 2. (a) Geometry of a metallic sphere covered with dielectric material in free-space. (b) The co-

polarized bi-static RCS ($\theta\theta$) of a metallic sphere covered with dielectric material for $0^\circ \le \theta_s \le 180^\circ, \phi_s = 0^\circ$ at 300MHz.

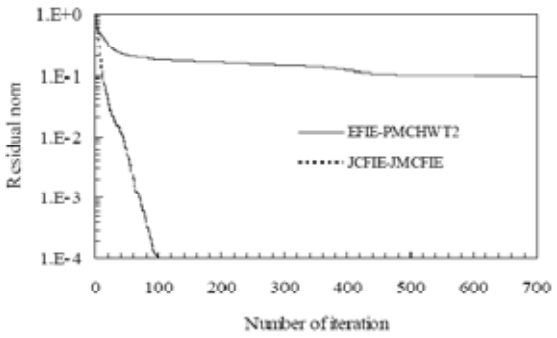

Fig. 3. The convergence history of JCFIE-JMCFIE, EFIE-PMCHWT2 solved with FGMRES for a metallic sphere covered with dielectric material in free-space at 300MHz.

Next, we extended the JCFIE-JMCFIE method to analyze the half-space problems to verify the accuracy and efficiency of the JCFIE-JMCFIE. As shown in Fig. 4(a), we consider a metallic sphere covered with spherical dielectric material situated 0.3577m above the lossy half space characterized by $\varepsilon_{half} = 5.0 - j0.2$ and $\mu_{half} = 1.0$. The metallic sphere's radius is $a_1 = 0.3423\lambda_0$. The thickness of the coated dielectric material is $a_2 = 0.1017\lambda_0$ and the relative permittivity is with $\varepsilon_r = 4$. The incident angles of plane wave are $\theta_i = 180^\circ$ and $\phi_i = 180^\circ$ at $f = 300MHz$. The metallic sphere coated with spherical dielectric is, also, discretized with 3240 triangular patches leading to 7720 unknowns. Figure 4(b) gives the bi-static RCS for the above half-space metallic sphere coated with spherical dielectric solved by the JCFIE-JMCFIE and EFIE-PMCHWT2, respectively. The scattering angle is $0^\circ \le \theta_s \le 90^\circ, \phi_s = 0^\circ$. The two levels MLFMA are used to accelerate the matrix-vector products. The simulated results obtained from the method of moment for bodies of revolution (BORMoM) and FEKO software are given to compare to them from JCFIE-JMCFIE and EFIE-PMCHWT2. In the BORMoM computation, the coated metallic sphere is discretized along the generating arc leading to 114 unknowns. The order of Fourier mode is 10 and the computation time is 2308.3 seconds in BORMoM. From Fig. 4(b), the results of JCFIE-JMCFIE and EFIE-PMCHWT2 agree well with the BORMoM and FEKO results. Furthermore, Fig. 5 gives the convergence rates of the JCFIE-JMCFIE and EFIE-PMCHWT2 formulations solved by the FGMRES method for the above half-space example. It is obvious that the application of the novel integral equation JCFIE-JMCFIE greatly accelerates the convergence rate compared with the EFIE-PMCHWT2 formulation.

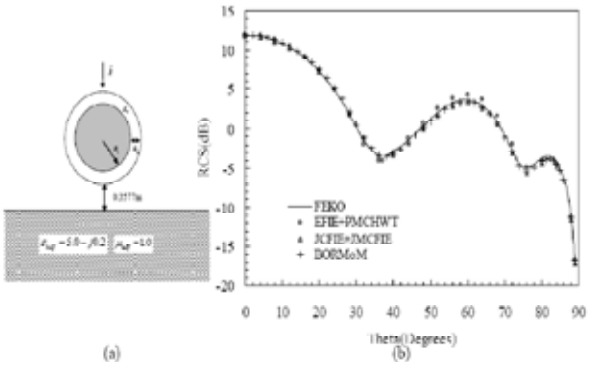

Fig. 4. (a) Geometry of a metallic sphere covered with spherical dielectric material situated above the lossy half space. (b) The co-polarized bi-static RCS ($\theta\theta$) of a metallic sphere covered with spherical dielectric material situated above the lossy half space for $0^\circ \le \theta_s \le 90^\circ, \phi_s = 0^\circ$ at 300MHz.

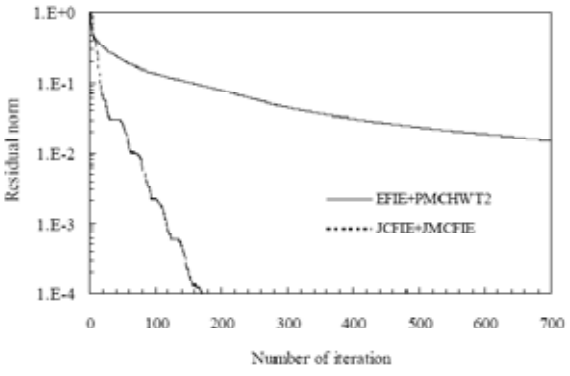

Fig. 5. The convergence history of JCFIE-JMCFIE, EFIE-PMCHWT2 solved with FGMRES for a metallic sphere covered with spherical dielectric material situated above the lossy half space at 300MHz.

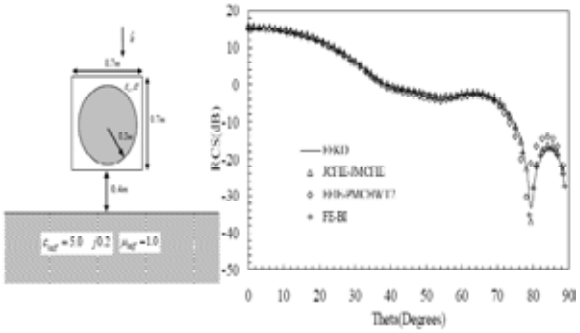

Fig. 6. (a) Geometry of a metallic sphere covered with cubic dielectric material situated above the lossy half space. (b) The co-polarized bi-static RCS ($\theta\theta$) of a metallic sphere covered with cubic dielectric material situated above the lossy half space for $0^\circ \le \theta_s \le 90^\circ, \phi_s = 0^\circ$ at 300MHz.

The another example shown in Fig. 6(a) is a metallic sphere covered with cubic dielectric situated 0.4 m above the lossy half space characterized by $\varepsilon_{half} = 5.0 - j0.2$ and $\mu_{half} = 1.0$. The metallic sphere's radius is 0.3m. The coated cubic dielectric is lossy. The conductivity and relative permittivity of dielectric are $\sigma = 0.001$s/m and $\varepsilon_r = 4$, respectively. The incident angles of plane wave are $\theta_i = 180^\circ$ and $\phi_i = 180^\circ$ at a frequency of $f = 300MHz$. The metallic sphere coated with spherical dielectric is also discretized with triangular patches leading to 10896 unknowns. Figure 6(b) gives the bi-static RCS for the above half-space metallic sphere coated with cubic dielectric solved by the JCFIE-JMCFIE, EFIE-PMCHWT2 finite element-boundary integral method (FE-BI) and FEKO software, respectively. The scattering angle is $0^\circ \le \theta_s \le 90^\circ, \phi_s = 0^\circ$. MLFMA with 2 levels is used to accelerate the matrix-vector products. In the FE-BI computation, the number of unknowns is 23651 and the computation time is 432.2 seconds. From Figure 6(b), it can be found that the results of JCFIE-JMCFIE are in good agreement with them obtained from EFIE-PMCHWT2, FE-BI and FEKO. Figure 7, also, shows the convergence rates of the JCFIE-JMCFIE and EFIE-PMCHWT2 formulations solved by FGMRES method for the last half-space example. It can be found that the proposed JCFIE-JMCFIE method only needs 139 iteration steps to reach convergence while the EFIE-PMCHWT2 method can not converge after 700 iteration steps.

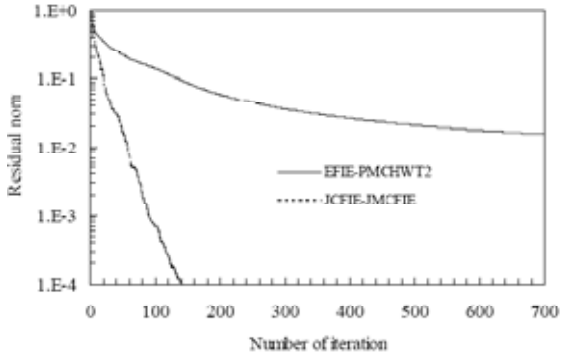

Fig. 7. The convergence history of JCFIE-JMCFIE, EFIE-PMCHWT2 solved with FGMRES for a metallic sphere covered with cubic dielectric material situated above the lossy half space at 300MHz.

In order to further investigate the performance of the proposed JCFIE-JMCFIE method, the above half-space metallic sphere coated with spherical dielectric material with the larger dielectric constants is considered. Figure 8 gives the co-polarized bi-static RCS of a metallic sphere covered with spherical dielectric material with $\varepsilon_r = 10$ and $\varepsilon_r = 12$ situated above the lossy half space solved by the JCFIE-JMCFIE. The simulated results obtained from BORMoM are given to compare to them from JCFIE-JMCFIE. In the BORMoM computation, the coated metallic spheres with $\varepsilon_r = 10$ and $\varepsilon_r = 12$ are both discretized along the generating arc leading to 114 unknowns. The order of Fourier mode is 20 and the computation time of BORMoM is 5128.3 seconds and 6340.1 seconds for $\varepsilon_r = 10$ and $\varepsilon_r = 12$ cases, respectively. The scattering angle is $0^\circ \le \theta_s \le 90^\circ, \phi_s = 0^\circ$. The two levels MLFMA is used to accelerate the matrix-vector products. Figure 9 and Fig. 10 give the convergence rates of the JCFIE-JMCFIE and EFIE-PMCHWT2 formulations solved by FGMRES method for the above half-space example with $\varepsilon_r = 10$ and $\varepsilon_r = 12$, respectively. It can be found that the JCFIE-JMCFIE method only needs 713 iteration steps to reach the convergence for the $\varepsilon_r = 10$ example, while the EFIE-PMCHWT2 method can only converge to the error of 0.1 after 2000 iteration.

For the $\varepsilon_r = 12$ example, the JCFIE-JMCFIE method can reach convergence after 5581 iteration steps, while the EFIE-PMCHWT2 method only converge to the error of 0.1 after 10000 iteration steps. This demonstrates the efficiency of the proposed JCFIE-JMCFIE method for the half-space metallic sphere coated with larger dielectric constants dielectric material.

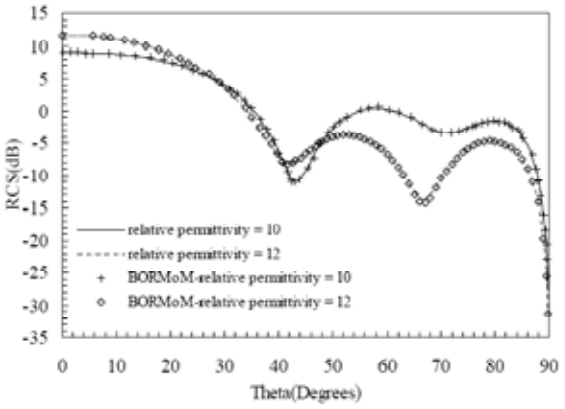

Fig. 8. The co-polarized bi-static RCS ($\theta\theta$) of a metallic sphere covered with spherical dielectric material with $\varepsilon_r = 10$ and $\varepsilon_r = 12$ situated above the lossy half space for $0^\circ \le \theta_s \le 90^\circ, \phi_s = 0^\circ$ at 300MHz.

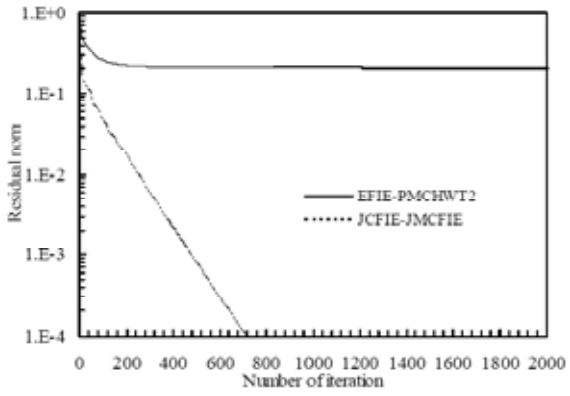

Fig. 9. The convergence history of JCFIE-JMCFIE, EFIE-PMCHWT2 solved with FGMRES for a metallic sphere covered with spherical dielectric material with $\varepsilon_r = 10$ situated above the lossy half space at 300MHz.

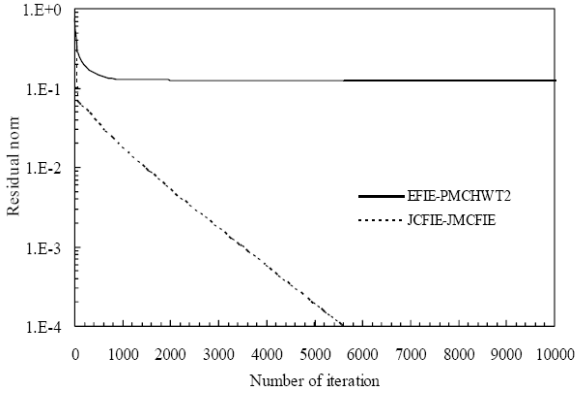

Fig. 10. The convergence history of JCFIE-JMCFIE, EFIE-PMCHWT2 solved with FGMRES for a metallic sphere covered with spherical dielectric material with $\varepsilon_r = 12$ situated above the lossy half space at 300MHz.

Figure 11 gives the convergence rates of the JCFIE-JMCFIE and EFIE-PMCHWT2 formulations solved by the FGMRES method for the above half-space metallic sphere covered with spherical dielectric material with $\varepsilon_r = 4$ in Figure 4(a). The metallic sphere coated with spherical dielectric is also discretized with triangular patches leading to 37302 unknowns. Due to the limit of computer memory (2GB RAM), larger problems (>40000) can not be computed. Furthermore, compared with the free-space MLFMA, aggregation and disaggregation for the image groups as well as calculations of the translation operator between image and observation group centers are additionally required during implementing half-space MLFMA in JCFIE-JMCFIE. As a result, the storage and CPU of half-space MLFMA are approximately twice that of a free-space MLFMA, due to the extra set of image clusters. From Figure 11, it can be found that the proposed JCFIE-JMCFIE method only needs 167 iteration steps to reach convergence while the EFIE-PMCHWT2 method can only converge to the error of 0.6 after 700 iteration steps.

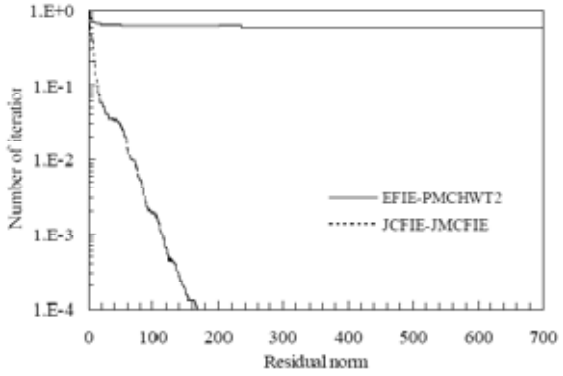

Fig. 11. The convergence history of JCFIE-JMCFIE, EFIE-PMCHWT2 solved with FGMRES for a metallic sphere covered with spherical dielectric material with situated above the lossy half space at 300MHz. The number of unknown is 37302.

Tables 1-3 list the iteration steps and computation time of the JCFIE-JMCFIE and EFIE+PMCHWT2 solved by FGMRES for above three examples where * refers to no convergence after maximum 20000 iterations. When compared in terms of solution time, the JCFIE-JMCFIE have a gain over the EFIE+PMCHWT2 by a factor of more than 160 on the first free-space example, 32.2 on the second half-space metallic sphere example coated with spherical dielectric, 61.9 on the third half-space metallic sphere example coated with cubic dielectric. It can be found that the JCFIE-JMCFIE reduces the computation time significantly while it maintains high accuracy when compared with the traditional EFIE+PMCHWT2.

IV. CONCLUSION

In this paper, a well-conditioned coupled surface integral equation called JCFIE-JMCFIE is proposed for the analysis of electromagnetic scattering from coated targets above a lossy half-space. The coupled formulation can lead to a well tested system with the RWG basis functions and Galerkin's method. To efficiently analyze electrically large scattering problems in half-space, the half-space MLFMA is implemented to reduce the computational complexity and memory requirement. The inner-outer FGMRES is used as the iterative solver to further enhance the convergence rate. Numerical results are demonstrated to validate the proposed method and show the accuracy and high efficiency compared with the traditional EFIE-PMCHWT2 method. Further investigations deserve to be undertaken to study the parallelization of the proposed JCFIE-JMCFIE with MLFMA.

Table 1: Comparison of the iteration steps and computation time of JCFIE-JMCFIE and EFIE-PMCHWT2 for the metallic sphere coated with spherical dielectric on free space

	Unknowns	Iteration steps	Computation time(s)
EFIE-PMCHWT2	7720	*	>20000
JCFIE-JMCFIE	7720	100	121.8

Table 2: Comparison of the iteration steps and computation time of JCFIE-JMCFIE and EFIE-PMCHWT2 for the metallic sphere coated with spherical dielectric situated 0.3577m above the lossy half space

	Unknowns	Iteration steps	Computation time(s)
EFIE-PMCHWT2	7720	9082	7054.16
JCFIE-JMCFIE	7720	173	219.28

Table 3: Comparison of the iteration steps and computation time of JCFIE-JMCFIE and EFIE-PMCHWT2 for the metallic sphere coated with cubic dielectric situated 0.4m above the lossy half space

	Unknowns	Iteration steps	Computation time(s)
EFIE-PMCHWT2	10896	16024	13559.17
JCFIE-JMCFIE	10896	139	219.28

ACKNOWLEDGMENT

The authors would like to thank the support of Natural Science Foundation of China under Contract Number 60701005, 60871013, Natural Science Foundation of Jangsu under Contact Number BK2009387, NUST Research Funding under Contract Number 2010ZYTS026, and the Research Fund for the Doctoral Program of Higher Education under Contract Number 20070288043.

REFERENCES

[1] N. Geng, A. Sullivan, and L. Carin, "Multilevel fastmultipole algorithm for scattering from conducting targets above or embedded in a lossy half space," *IEEE Trans. Geosci. Remote Sensing*, vol. 38, no. 4, pp. 1561-1573, July 2000.

[2] Z. J. Liu, J. Q. He, Y. J. Xie, A. Sullivan, and L. Carin, "Multi-level fast multipole algorithm for general targets on a half-space interface," *IEEE Trans. on Antenna and Propagation*, vol. 50, no. 12, pp. 1838-1849, Dec. 2002.

[3] L. Li, J. Q. He, Z. J. Liu, X. L. Dong, and L. Carin, "MLFMA analysis of scattering from multiple targets in the presence of a half-space," *IEEE Trans. on Antenna and Propagation*, vol. 51, no. 4, pp. 810-819, Apr. 2003.

[4] N. Geng, A. Sullivan, and L. Carin, "Fast multipole method for scattering from an arbitrary PEC target above or buried in a lossy half space," *IEEE Trans. on Antenna and Propagation*, vol. 49, no. 5, pp. 740-748, May 2001.

[5] D. Z. Ding, R. S. Chen, and Z. H. Fan, "Application of two-step spectral preconditioning technique for electromagnetic scattering in half-space," *Progress In Electromagnetics Research*, PIER 94, pp. 383-402, 2009.

[6] R. F. Harrington, *Field Computation by Moment Methods*, Malabar, Fla.: R. E. Krieger, 1968.

[7] S. M. Rao, D. R. Wilton, and A. W. Glisson, "Electromagnetic scattering by surfaces of arbitrary shape," *IEEE Trans. on Antenna and Propagation*, vol. 30, no. 3, pp. 409-418, 1982.

[8] W. C. Chew, J. M. Jin, E. Midielssen, and J. M. Song, *Fast and Efficient Algorithms in Computational Electromagnetics*. Boston, MA: Artech House, 2001.

[9] D. Z. Ding, R. S. Chen, and Z. H. Fan, "An Efficient SAI Preconditioning Technique For Higher Order Hierarchical MLFMM Implementation", *Progress In Electromagnetics Research*, PIER 88, pp. 255-273, 2008.

[10] D. Z. Ding, R. S. Chen, Z. H. Fan and P.L. Rui, "A Novel Hierarchical Two-level Spectral Preconditioning Technique for Multilevel Fast Multipole Analysis of Electromagnetic Wave Scattering," *IEEE Trans. on Antenna and Propagation*, vol. 56, no. 4, pp. 1122-1132, April 2008.

[11] Ö. Ergül, and L. Gürel, "Linear-linear Basis Functions for MLFMA Solutions of Magnetic-Field and Combined-Field Integral Equations," *IEEE Trans. on Antenna and Propagation*, vol. 55, no. 4, pp. 1103-1110, April 2007.

[12] R. M. Shubair, and Y. L. Chow, "A simple and accurate complex image interpretation of vertical antennas present in contiguous dielectric half-spaces," *IEEE Trans. on Antenna and Propagation*, vol. 41, pp. 806-812, June 1993.

[13] M. I. Aksun, "A robust approach for the derivation of closed-form Green's functions," *IEEE Trans. Microwave Theory and Technique*, vol. 44, pp. 651–658, May 1996.

[14] N. A. Geng, Sullivan, and L. Carin, "Fast multipole method for scattering from 3D PEC targets situated in a half-space environment," *Microw. Opt. Technol. Lett.*, vol. 21, pp. 399-405, June 1999.

[15] X. Q. Sheng, J. M. Jin, J. M. Song, W. C. Chew, and C. C. Lu, "Solution of Combined-Field Integral Equation Using Multilevel Fast Multipole Algorithm for Scattering by Homogeneous Bodies," *IEEE Trans. Antennas Propagat.*, vol. 46, no. 11, pp. 1718 -1726, November 1998.

[16] P. Ylä-Oijala and Matti Taskinen, "Application of Combined Field Integral Equation for Electromagnetic Scattering by Dielectric and Composite Objects," *IEEE Trans. Antennas Propagat.*, vol. 53, no. 3, pp. 1168–1173, March 2005.

[17] P. Ylä-Oijala, M. Taskinen, and S. Järvenpää, "Analysis of surface integral equations in electromagnetic scattering and radiation problems," *Engineering Analysis with Boundary Elements*, vol. 32, pp. 196-209, 2008.

[18] S. M. Rao, C. C. Cha, R. L. Cravey, and D. L. Wilkes, "Electromagnetic Scattering from Arbitrary Shaped Conducting Bodies Coated with Lossy Materials of Arbitrary Thickness," *IEEE Trans. Antennas Propagat.*, vol. 39, no. 5, pp. 627-631, May 1991.

[19] Ö. Ergül and L. Gürel, "Comparison of Integral-Equation Formulations the Fast and Accurate Solution of Scattering Problems Involving Dielectric Objects with the Multilevel Fast Multipole Algorithm," *IEEE Trans. Antennas Propagat.*, vol. 57, no. 1, pp. 176-187, Jan. 2009.

[20] Ö. Ergül and L. Gürel, "Discretization Error Due to the Identity Operator in Surface Integral Equations," *Computer Physics Communications,* vol. 180, pp. 1746 – 1752, 2009.

[21] Y. Saad, *Iterative methods for sparse linear systems*, PWS Publishing Company, 1996.

[22] Y. Saad and M. H. Schultz, "GMRES: A generalized minimal residual algorithm for solving nonsymmetric linear systems," *SIAM J Sci Statist Comput*, vol. 7, pp. 856 – 869, 1986.

[23] D. Z. Ding, R. S. Chen, Z. H. Fan, Edward K. N. Yung, and C.H. Chan, "Fast analysis of electromagnetic scattering of 3D dielectric bodies by use of the loose GMRES-FFT method," *International Journal of Electronics*, vol. 92, no. 7, pp. 401-415, July 2005.

[24] D. Z. Ding, R. S. Chen, D. X. Wang, W. Zhuang, and Edward K. N. Yung, "Application of the inner-outer flexible GMRES-FFT method to the analysis of scattering and radiation by cavity-backed patch antennas and arrays," *International Journal of Electronics*, vol. 92, no. 11, pp. 645-659, Nov. 2005.

[25] K. A. Michalski and D. Zheng, "Electromagnetic scattering and radiation by surfaces of arbitrary shape in layered media, Parts I and II," *IEEE Trans. on Antenna and Propagation*, vol. 38, pp. 335-352, Mar. 1990.

Dazhi Ding was born in Jiangsu, the People's Republic of China in 1979. He received the B.S. and Ph.D. degrees in Electromagnetic Field and Microwave Technique from Nanjing University of Science and Technology (NUST), Nanjing, China, in 2002 and 2007, respectively. During 2005, he was with the Center of Wireless Communication in the City University of Hong Kong, Kowloon, as a Research Assistant. He is currently an Associate Professor with the Electronic Engineering of NJUST. He is the author or coauthor of over 30 technical papers. His current research interests include computational electromagnetics, electromagnetic scattering, and radiation.

Jinmin Ge was born in Shandong Province, China, in 1987. She received the B.S. degree in Electrical Engineering from Huaiyin Normal University, Huaiyin, China, in 2007. She received the Master's degree in Nanjing University of Science and Technology (NUST), Nanjing, China, in 2009. Her current research interests include computational electromagnetics, antennas, and electromagnetic scattering, and propagation.

Rushan Chen was born in Jiangsu, China in 1965. He received the B.Sc. and M.Sc. degrees from Southeast University, Nanjing, China, in 1987 and 1990, respectively, and the Ph.D. degree in from Electronic Engineering from City University of Hong Kong, Kowloon, in 2001. In September 1999, he was promoted to Full Professor. His research interests mainly include microwave/millimeter-wave systems, measurements, antenna, RF-integrated circuits, and computational electromagnetics. He is the recipient of the Foundation for China Distinguished Young Investigators presented by the National Science Foundation (NSF) of China in 2003. In 2008, he became a Chang-Jiang Professor under the Cheung Kong Scholar Program awarded by the Ministry of Education, China.